Advances in Computational Design, *Vol. 6, No. 4 (2021) 329-338*
https://doi.org/10.12989/acd.2021.6.4.329

The damped vibration of the annular and rectangular graded beams in the presence of the attached lumped mass

Abbas Heydari*

Department of Civil Engineering, Technical and Vocational University (TVU), Tehran, Iran

(Received July 8, 2021, Revised September 17, 2021, Accepted September19, 2021)

Abstract. In earthquake engineering, vibration control is a set of engineering tools aimed at mitigating seismic effects on structural members. Once the seismic waves have penetrated a building, there are a number of ways to control them to mitigate their damaging effects and improve the seismic performance of the building. Dissipate the wave energy inside the structure with properly designed dampers, distributing the wave energy over a wider frequency range and absorbing the resonant portions of the entire wave frequency band using what are known as mass dampers. The effect of mass attenuator on the reduction of fundamental frequency of beams made of functionally graded material (FGM) with annular and rectangular cross sections is studied. Mori-Tanaka homogenization scheme, conventional mixing rule and power law functions are used to model the material gradation. Various classical boundary conditions as well as shear hinge natural condition are considered. The lumped mass attenuator is connected to the beam at an arbitrary position without sliding. The total potential energy is minimized by using the spectral Ritz method to calculate the fundamental frequency and the corresponding mode shape. A reduction in the frequencies is observed in the presence of the attached lumped mass attenuator. The dimensionless frequency reduction is affected by the amount and position of the lumped mass. The position of the lumped mass attenuator plays an important role in vibration control of the beam.

Keywords: classical beam theory; lumped mass damper; material gradation; spectral ritz method; vibration analysis

1. Introduction

In earthquake engineering, vibration control is a set of engineering tools aimed at mitigating seismic effects on buildings and other structures. Passive control devices have no feedback capability between them, structural elements, and the ground. The active control devices include real-time ground recording instruments integrated with earthquake input processing devices and actuators within the structure and hybrid control devices combine the features of active and passive control systems. Once the seismic waves have penetrated a building, there are a number of ways to control them to mitigate their damaging effects and improve the seismic performance of the building. Dissipate the wave energy inside the structure with properly designed dampers, distributing the wave energy over a wider frequency range and absorbing the resonant portions of

*Corresponding author, Assistant Professor, E-mail: a_heydari@tabrizu.ac.ir

http://www.techno-press.org/?journal=acd&subpage=7 ISSN: 2383-8477 (Print), 2466-0523 (Online)

the entire wave frequency band using what are known as mass dampers.

For passive vibration control, the nonlinear vibration absorbers are studied in detail. The exact nonlinear dynamics of a simply supported beam carrying a nonlinear spring-inerter-damper energy absorber to reduce primary resonant vibration reduction is investigated. For this purpose, the analytical model and nonlinear dynamic responses for a beam-spring-inerter-damper system are derived (Zuo and Qian 2021). The effects of sand size and volume fraction on the damping of free vibration of a beam are investigated. A high-speed camera was used to measure the damping ratio of the beam vibration. It is found that the damping ratio for partially filled beams is larger than that for completely filled and empty beams. It is also found that the maximum damping ratio occurs at different mass fractions (Hashemnia 2021). The vibration control of a rotating beam made of functional gradient material (FGM) under thermal conditions is investigated using an enhanced active constrained layer damping (EACLD) method. The mentioned model is an extension of a newly developed dynamic model for EACLD composite beams. The difference is that the base beam is made of temperature-dependent FGM, which is widely used in the aerospace industry as an advanced heat-resistant composite material, and the temperature dependence of the viscoelastic material in the constrained layer is also considered (Fang *et al*. 2021). The effect of edge relaxation on the free vibration properties of a rotating laminated Timoshenko composite beam is investigated. Based on the first-order shear theory, the theoretical model of the rotating laminated Timoshenko composite beam is established, in which the possion effect is also considered. The relaxed boundary conditions of the beam are simulated with a series of artificial springs. By adjusting the stiffness of the springs, varying degrees of relaxed boundary conditions of the beam can be obtained. Relaxation parameters are introduced to evaluate the extent of boundary relaxation. A unified formula for the centrifugal force of the rotating beam with relaxed boundary conditions is derived (Xu *et al*. 2021). The vibration characteristics of a cantilever L-shaped beam perpendicular to the horizontal plane are investigated. The dynamic model of the L-shaped multicarrier structure is established using Euler-Bernoulli beam theory, including the vibration equations of each substructure, the fitting conditions of the connection and the boundary conditions. Based on the modal orthogonality, a discrete dynamic model with finite degrees of freedom is established. Then the distributed piezoelectric energy harvester is proposed to collect the vibration energy of the L-shaped beam (Cao *et al*. 2021). The eigensolutions of the non-viscous damped systems are performed based on the fixed point iteration (Lázaro 2018). The smart damping layer under a plate subjected to a pair of masses moving in opposite directions is elaborated (Bajer *et al*. 2017). The boundary friction damping (Yang *et al*. 2019), vibration problems of composite shells (Kiani *et al*. 2018) and plates (Rani and Lal 2019) and optimization problem of composite structures under vibration and buckling loads (Akbulut *et al*. 2020) are studied. The many relevant works can be found in literature (She *et al*., 2021, Zhang *et al*. 2021, Lu *et al*. 2021, Heydari and Shariati 2018, Heydari *et al*. 2017, Heydari 2018, Heydari 2018, Heydari 2015, Heydari 2013, Heydari and Jalali 2017, Heydari and Li 2021, Heydari 2020).

In the present work, the effect of the position of the lumped mass damper on the reduction of the fundamental frequency of the FGM beam with annular and rectangular cross sections is investigated. The volume fraction distribution of the functionally graded material is used to model the mass density. The lumped mass is connected to the beam at an arbitrary position without sliding. The FGM beam has a small thickness to length ratio, so the total potential energy is derived based on Euler-Bernoulli beam theory. The total potential energy is minimized by applying the spectral Ritz method to calculate the fundamental frequency and the corresponding mode shape. The various classical boundary conditions including simply supported beam, clamped

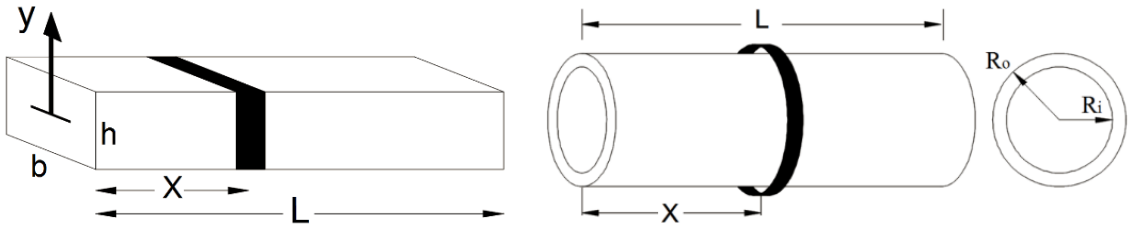

(a) transversly (b) radially graded

Fig. 1 The FGM beam with lumped mass damper

beam, pinned-clamped beam and cantilever beam as well as shear hinge natural condition are considered. A reduction in frequencies is observed in the presence of a lumped mass damper. However, the dimensionless frequency reduction is a function of the amount and position of the lumped mass, but the position of lumped mass has a more important effect on the vibration control of the functionally graded beam. Convergence of numerical results is observed by using small terms in the basis.

2. Vibration Analysis

The Fig. 1 illustrates a functionally graded beam and an attached lumped mass damper. The length, width and height of the beam are L, b and h respectively. The position of the lumped mass damper is measured from the left end of the FGM beam. The mass of the ring will be considered in terms of the total mass of the FGM beam.

The total potential energy of the functionally graded beam and connected lumped mass, m, at position X from left end of the beam is written as follows:

$$\Pi = \frac{1}{2}\int_0^L \left(EI_{eq}(w'')^2 - \bar{m}_{eq}w^2\omega^2\right)dx - \frac{1}{2}m(w|_{x=X}\omega)^2, \tag{1}$$

where, EI_{eq} and $\bar{m}_{eq}$ are equivalent flexural rigidity and equivalent mass per unit length of the functionally graded beam. The deflection of the FGM beam is w. The parameter ω denotes natural angular frequency of the free vibration. In the Mori–Tanaka homogenization scheme the effective bulk modulus, K_e, and effective shear modulus, μ_e, can be calculated from Eqs. (2) and (3).

$$\frac{K_e - K_m}{K_c - K_m} = \frac{V_c}{1 + \dfrac{V_m(K_c - K_m)}{K_m + \dfrac{4\mu_m}{3}}} \tag{2}$$

$$\frac{\mu_e - \mu_m}{\mu_c - \mu_m} = \frac{V_c}{1 + \dfrac{V_m(\mu_c - \mu_m)}{\mu_m + \dfrac{\mu_m(9K_m + 8\mu_m)}{6K_m + 12\mu_m}}} \tag{3}$$

The effective modulus of elasticity and Poisson's ratio are

$$E(y) = \frac{9K_e\mu_e}{3K_e + \mu_e}, \tag{4}$$

$$\nu(y) = \frac{3K_e - 2\mu_e}{6K_e + 2\mu_e} \tag{5}$$

The distance between neutral axis position and mid-axis position is e. As a result, one can write

$$EI_{eq} = b\int_{-\frac{h}{2}-e}^{\frac{h}{2}-e}\left(\frac{9K_e\mu_e}{3K_e + \mu_e}\right)y^2 dy \tag{6}$$

The parameter e can be obtained as follows:

$$e = \frac{\int_{-\frac{h}{2}}^{\frac{h}{2}} E(y) \times y dy}{\int_{-\frac{h}{2}}^{\frac{h}{2}} E(y) dy} \tag{7}$$

The mass density distribution of the FGM beam is assumed as follows:

$$\rho(y) = \rho_m V_m + \rho_c V_c \tag{8}$$

in which, ρ_m and ρ_c are mass density of the metal and ceramic constituents, respectively. The volume fraction of the phase materials are

$$V_c = \left(\frac{y}{h} + \frac{1}{2}\right)^n \tag{9}$$

$$V_m = 1 - \left(\frac{y}{h} + \frac{1}{2}\right)^n \tag{10}$$

where n is gradient index or material exponent parameter which takes non-negative real numbers. The linear mass density of the FGM beam is calculated as follows:

$$m_{eq} = b\int_{-\frac{h}{2}}^{\frac{h}{2}} \rho(y) dy, \tag{11}$$

The variation of the elasticity modulus in FGM tube is modeled via power law function as follows:

$$E(r) = E_0 r^n, \tag{12}$$

in which, E_0 and n are material constants. Because of the axisymmetric distribution of material, the neutral axis position coincides with mid-axis position. As a result, one can write

$$EI_{eq} = \int_0^{2\pi}\int_{R_i}^{R_o} E_0 r^n (r\sin\theta)^2 \, r dr d\theta, \tag{13}$$

The solution of the integration in Eq. (13) is

$$EI_{eq} = \begin{cases} \dfrac{\pi\left(R_o^{n+4} - R_i^{n+4}\right)}{n+4} & n \neq -4 \\ \pi \ln\left(\dfrac{R_o}{R_i}\right) & n = -4 \end{cases}, \tag{14}$$

The mass density distribution of the FGM tube is assumed as follows:

$$\rho(r) = \rho_0 r^q, \tag{15}$$

in which, ρ_0 and q are material constants. The linear mass density of the FG tube is calculated as follows:

$$m_{eq} = \int_0^{2\pi} \int_{R_i}^{R_o} \rho_0 r^q \, r dr d\theta, \tag{16}$$

The solution of the integration in Eq. (16) is

$$m_{eq} = \begin{cases} \dfrac{2\pi\rho_0\left(R_o^{q+2} - R_i^{q+2}\right)}{q+2} & q \neq -2 \\ 2\pi\rho_0 \ln\left(\dfrac{R_o}{R_i}\right) & q = -2 \end{cases}, \tag{17}$$

The spectral Ritz method is applied to calculate first frequencies of the system. The truncated Taylor series expansion of the deflection is selected as basis function and unknown coefficients.

$$w = \bar{w} + \sum_{k=4}^{N} c_k x^k, \tag{18}$$

The function $\bar{w}$ includes the coefficients c_0 to c_3. After satisfying boundary and natural conditions, the coefficients c_0 to c_3 are calculated in terms of the remaining coefficients c_4 to c_N, consequently Eq.(12) is the general form of the deflection function for various end conditions of the FGM beam. For example, the function $\bar{w}$ is calculated by satisfying $w(0) = w'(0) = w'(L) = W'''(L) = 0$ for clamped-shear hinge end FGM beam. Substituting Eq. (18) into Eq. (1), one has

$$\Pi = f(c_4, c_5, \dots, c_N), \tag{19}$$

Minimizing total potential energy, yields

$$\frac{\partial \Pi}{\partial c_i} = 0 \qquad 4 \leq i \leq N, \tag{20}$$

The characteristic equation will be obtained by considering nontrivial solution. To this purpose, determinant of the matrix of the coefficients must be vanished. The matrix of the coefficients is Hessian of the total potential energy.

$$\left|H_{ij}\right| = \left|\frac{\partial^2 \Pi}{\partial c_i \partial c_j}\right| = 0 \qquad 4 \leq i \leq N, 4 \leq j \leq N, \tag{21}$$

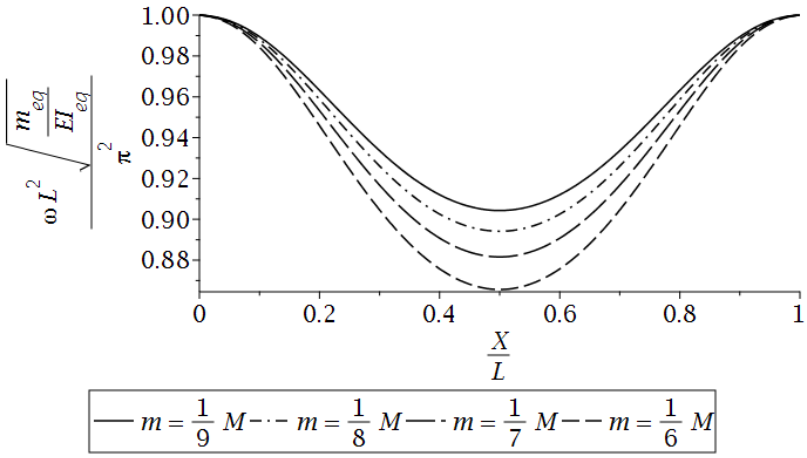

Fig. 2 Dimensionless fundamental frequency of the simply supported FGM beam

After substituting angular frequency of damped vibration into Hessian of the total potential energy, $[H]$, the unknowen coefficients can be calculated in terms of an arbitrary coefficient, say c_N, as follows:

$$\begin{Bmatrix} a_1 \\ \vdots \\ a_{N-1} \end{Bmatrix} = -a_N [H^*]^{-1} \{\tilde{H}\} \qquad 4 \le i \le N, 4 \le j \le N, \tag{22}$$

The square matrix $[H^*]$ is calculated by deleting last row and last column of the matrix $[H]$. For calculating the vector $\{\tilde{H}\}$, the last row of the matrix $[H]$ is deleted, afterwards the last column of the remained matrix is considered.

Instead of a truncated Taylor series expansion of the deflection, one can use orthogonal polynomials such as the Legendre polynomials, which have a high rate of convergence. A set of elements in a space with inner product is orthogonal if the inner product of each pair of distinct elements is zero. A set of vectors in a space with inner product is orthogonal to another set if the inner product of every vector of the first set with every vector of the second set is zero. An orthogonal set in which the inner product of each element is one with itself is called orthonormal. A set of functions f_1,..., f_n (that may be infinite), of which every pair of distinct functions satisfies the identity

$$\int_a^b \bar{w}(x) f_i(x) f_j(x)\, dx = \ 0 \tag{23}$$

where $\bar{w}(x)$ is a weight function, on some given range of integration]a, b[, or for a more general set and measure. The complete set of orthogonal polynomials, $P_i(x)$, on [-1, 1], and defined by $P_0 \ = \ 1$, and

$$P_n(x) = \frac{1}{2^n n!} \frac{d^n}{dx^n} (x^2 - 1)^n \tag{24}$$

The n^{th} polynomial, for which this is Rodrigues' formula, solves Legendre's differential equation with $p \ = \ n$.

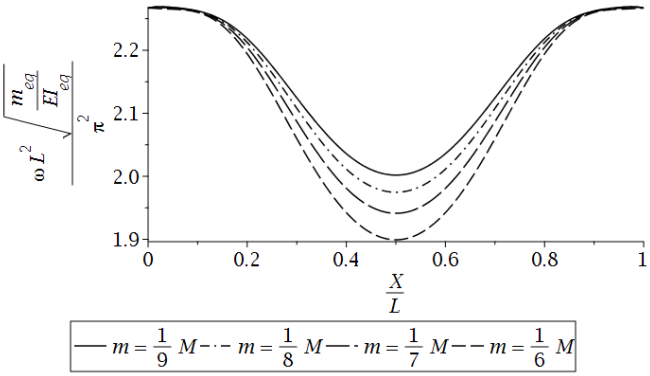

Fig. 3 Dimensionless fundamental frequency of the clamped FGM beam

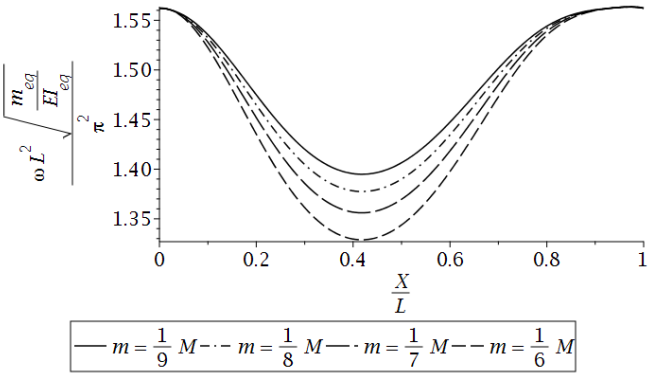

Fig. 4 Dimensionless fundamental frequency of the pinned-clamped FGM beam

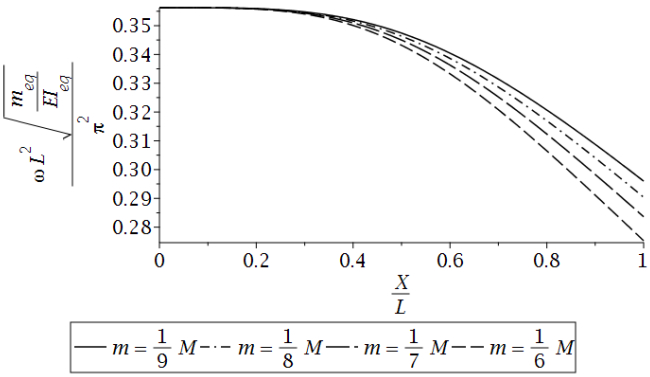

Fig. 5 Dimensionless fundamental frequency of the cantilever FGM beam

3. Results and discussion

The dimensionless fundamental angular frequency of the free vibration for simply supported FGM beam with various amounts of lumped mass against the position of the lumped mass is presented in Fig. (2). The parameter M is the total mass of the FGM beam ($M = \bar{m}_{eq}L$). The

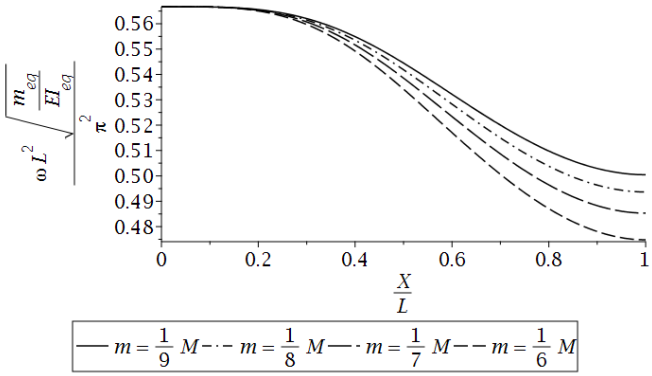

Fig. 6 Dimensionless fundamental frequency of the clamped-shear hinge end FGM beam

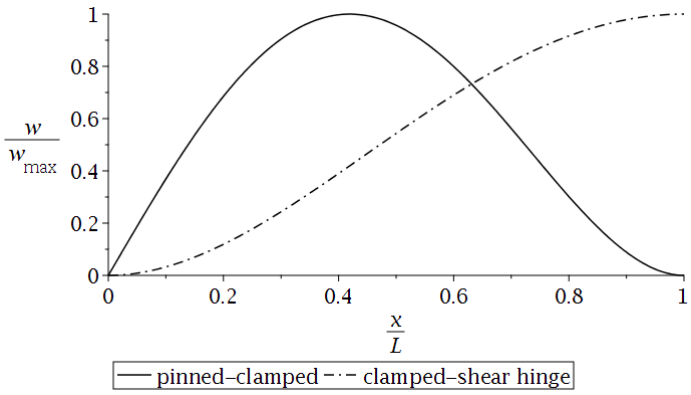

Fig. 7 First mode shape of the FGM beam

dimensionless fundamental angular frequency of FGM beam for various amounts of lumped mass and various boundary conditions against the position of the lumped mass is presented in Fig. (3) to Fig. (6).

Fig. (2) to Fig. (6) show that the shape of the fundamental frequency reduction curve is similar to the shape of the first mode of the FGM beam. For example, first mode shapes of the pinned-clamped and clamped- shear hinge end FGM beams are presented in Fig. (7).

4. Conclusions

The effect of the position of the attached lumped mass on the frequency reduction of the FGM beam with different cross sections and different material distributions is investigated. The equivalent linear mass density and equivalent bending stiffness of the FGM beam are calculated. The results for different end conditions are presented. The dimensionless fundamental frequency decreases with increasing amount of connected lumped mass. It is shown that the decrease in natural frequency is a function of the amount and position of the lumped mass. The shape of the frequency reduction diagram is similar to the mode shape of the FGM beam. The position of the attached lumped mass can be used for vibration control of the FGM beam. In the present work, the

attached lumped mass position for frequency reduction is proposed for the first time. This new concept can be used as a new device for vibration control of cantilever beams.

References

Akbulut, M., Sarac, A. and Ertas, H.A., (2020), "An investigation of non-linear optimization methods on composite structures under vibration and buckling loads", *Advan. Comput. Des.*, **5**(3), 209-231. http://dx.doi.org/10.12989/acd.2020.5.3.209.

Bajer, C., Pisarski, D., Szmidt, T. and Dyniewicz B., (2017), "Intelligent damping layer under a plate subjected to a pair of masses moving in opposite directions", *J. Sound Vib.*, **394**(28), 333-347. https://doi.org/10.1016/j.jsv.2017.01.046.

Cao, Y., Cao, D., He, G., Ge, X. and Hao, Y. (2021), "Vibration analysis and distributed piezoelectric energy harvester design for the L-shaped beam", *Europ. J. Mech. - A/Solids*, **87**, 104214. https://doi.org/10.1016/j.euromechsol.2021.104214.

Fang, Y., Lia, L., Zhang, D., Chen, S. and Liao, W. (2021), "Vibration suppression of a rotating functionally graded beam with enhanced active constrained layer damping treatment in temperature field", *Thin-Wall. Struct.* **161**, 107522. https://doi.org/10.1016/j.tws.2021.107522.

Hashemnia, K. (2021), "Effect of particle size and media volume fraction on the vibration attenuation of a thin-walled beam containing granular media", *Soil Dyn. Earthq. Eng.* **147**, 106816. https://doi.org/10.1016/j.soildyn.2021.106816.

Heydari, A. (2013), "Analytical solutions for buckling of functionally graded circular plates under uniform radial compression using Bessel function", *Int. J. Advan. Des. Manufact. Technol.*, **6**, 4, 41-47.

Heydari, A. (2015), "Spreading of plastic zones in functionally graded spherical tanks subjected to internal pressure and temperature gradient combinations", *Iran. J. Mech. Eng.*, **16**(2), 5-25.

Heydari, A. (2018), "Exact vibration and buckling analyses of arbitrary gradation of nano-higher order rectangular beam", *Steel Compos. Struct.*, **28**(5), 589-606. https://doi.org/10.12989/scs.2018.28.5.589.

Heydari, A. (2018), "Size-dependent damped vibration and buckling analyses of bidirectional functionally graded solid circular nano-plate with arbitrary thickness variation", *Struct. Eng. Mech.* **68**(2), 171-182. http://dx.doi.org/10.12989/sem.2018.68.2.171.

Heydari, A. (2020), "Buckling analysis of discontinues fractional axially graded thin beam with piecewise axial load function rested on rotational spring hinges", *Int. J. Advan. Des. Manufact. Technol.*, **13**(2), 99-108.

Heydari, A. and Jalali, A. (2017), "A new scheme for buckling analysis of bidirectional functionally graded Euler beam having arbitrary thickness variation rested on Hetenyi elastic foundation", *Modares Mech. Eng.*, **17**, 1, 47-55.

Heydari, A. and Li, L. (2021), "Dependency of critical damping on various parameters of tapered bidirectional graded circular plates rested on Hetenyi medium", *Proceedings of the Institution of Mechanical Engineers, Part C: Journal of Mechanical Engineering Science*, **235**(12), 2157-2179. https://doi.org/10.1177/0954406220952498.

Heydari, A. and Shariati, M. (2018), "Buckling analysis of tapered BDFGM nano-beam under variable axial compression resting on elastic medium", *Struct. Eng. Mech.*, **66**(6), 737-748. http://dx.doi.org/10.12989/sem.2018.66.6.737.

Heydari, A., Jalali, A. and Nemati, A. (2017), "Buckling analysis of circular functionally graded plate under uniform radial compression including shear deformation with linear and quadratic thickness variation on the Pasternak elastic foundation", *Appl. Mathem. Modelling*, **41**, 494-507. https://doi.org/10.1016/j.apm.2016.09.012.

Kiani Y., Dimitri R. and Tornabene F. (2018), "Free vibration of FG-CNT reinforced composite skew cylindrical shells using the Chebyshev-Ritz formulation", *Compos. Part B: Eng.*, **147**, 169-177. https://doi.org/10.1016/j.compositesb.2018.04.028.

Lázaro M. (2018), "Eigensolutions of nonviscously damped systems based on the fixed-point iteration", *J. Sound Vib.*, **418**, 100-121. https://doi.org/10.1016/j.jsv.2017.12.025.

Lu, L., She, G.L. and Guo, X. (2021), "Size-dependent postbuckling analysis of graphene reinforced composite microtubes with geometrical imperfection", *Int. J. Mech. Sci.*, **199**, 106428. https://doi.org/10.1016/j.ijmecsci.2021.106428.

Rani R. and Lal R. (2019), "Free vibrations of composite sandwich plates by Chebyshev collocation technique», *Compos. Part B: Eng.*, **165**, 442-455. https://doi.org/10.1016/j.compositesb.2019.01.088.

She, G.L., Liu, H.B. and Karami, B. (2021), "Resonance analysis of composite curved microbeams reinforced with graphene nanoplatelets", *Thin-Wall. Struct.*, **160**, 107407. https://doi.org/10.1016/j.tws.2020.107407.

Xu, J., Yang, Z., Yang, J. and Li, Y. (2021), "Influence of the boundary relaxation on the free vibration of rotating composite laminated Timoshenko beams", *Compos. Struct.*, **266**, 113690. https://doi.org/10.1016/j.compstruct.2021.113690.

Yang Y., Jézéquel L., Dessombz O., Bristiel P. and Sauvage O. (2019), "Modelization of boundary friction damping induced by second-order bending strain", *J. Sound Vib.*, **446**, 113-128. https://doi.org/10.1016/j.jsv.2019.01.033.

Zhang, Y.Y., Wang, X.Y., Zhang, X., Shen, H.M. and She, G.L. (2021), "On snap-buckling of FG-CNTR curved nanobeams considering surface effects", *Steel Compos. Struct.*, **38**(3), 293-304. https://doi.org/10.12989/scs.2021.38.3.293.

Zuo, L. and Qian, F., (2021), "Tuned nonlinear spring-inerter-damper vibration absorber for beam vibration reduction based on the exact nonlinear dynamics model", *J. Sound Vib.*, **509**. https://doi.org/10.1016/j.jsv.2021.116246.

WT